CONSTRAINING THE SPIN OF THE BLACK HOLE IN FAIRALL 9 WITH *SUZAKU*

S. SCHMOLL[1], J. M. MILLER[1], M. VOLONTERI[1], E. CACKETT[1,9], C. S. REYNOLDS[2], A. C. FABIAN[3], L. W. BRENNEMAN[4,10],
G. MINIUTTI[5,6,7], AND L. C. GALLO[8]

[1] Department of Astronomy and Astrophysics, University of Michigan, 500 Church Street, Ann Arbor, MI 48109, USA; schmoll@umich.edu
[2] Department of Astronomy, The University of Maryland, College Park, MD 20742, USA
[3] Institute of Astronomy, University of Cambridge, Madingley Road, Cambridge CB3 OHA, UK
[4] NASA GSFC, mail code 662, Greenbelt, MD 20771, USA
[5] Max-Plack-Institut für extraterrestrische Physik, Postfach 1312, 85741 Garching, Germany
[6] Laboratoire APC, UMR 7164, 10 rue A. Domon et L. Duquet, 75205 Paris Cedex 13, France
[7] LAEX, Centro de Astrobiologia (CSIC-INTA), LAEFF, P.O. Box 78, E-28691, Villanueva de la Canada, Madrid ES, Spain
[8] Department of Astronomy and Physics, Saint Mary's University, 923 Robie Street, Halifax NS B3H 3CS, Canada
Received 2009 June 1; accepted 2009 August 7; published 2009 September 17

ABSTRACT

We report on the results of spectral fits made to data obtained from a 168 ks *Suzaku* observation of the Seyfert 1 galaxy Fairall 9. The source is clearly detected out to 30 keV. The observed spectrum is fairly simple; it is well described by a power law with soft excess and disk reflection. A broad iron line is detected, and easily separated from distinct narrow components owing to the resolution of the CCDs in the X-ray Imaging Spectrometer (XIS). The broad line is revealed to be asymmetric, consistent with a disk origin. We fit the XIS and Hard X-ray Detector spectra with relativistically blurred disk reflection models. With the assumption that the inner disk extends to the innermost stable circular orbit, the best-fit model implies a black hole spin parameter of $a = 0.60 \pm 0.07$ and excludes extremal values at a high level of confidence. We discuss this result in the context of Seyfert observations and models of the cosmic distribution of black hole spin.

Key words: accretion, accretion disks – black hole physics – galaxies: active – relativity – X-rays: galaxies

1. INTRODUCTION

The centers of active galactic nuclei (AGNs) contain a supermassive black hole (SMBH) that acts as the central engine by actively accreting matter. A topic of intensive study in AGN research is the radio-loud/radio-quiet dichotomy in the Eddington ratio/radio-luminosity plane (Sikora et al. 2007). There is an apparent morphological distinction with radio-loud galaxies only hosted by ellipticals, while radio-quiet galaxies are found to be either ellipticals or spirals. Theoretical work on this problem has suggested that SMBH spin may be a major contributor to determining if a galaxy is radio-loud or radio-quiet. Such models invoke the Blandford–Znajek effect to extract spin energy from the hole in order to power the radio jets (Blandford & Znajek 1977).

Astrophysical black holes have only two properties: mass and spin. It is likely that all black holes spin on some level; spin can be described by a dimensionless parameter defined as $\hat{a} = cJ/GM^2$, where J is the angular momentum of the black hole and $0 < \hat{a} < 0.998$ (Thorne 1974). Spin is a constantly evolving parameter for a black hole because every time it accretes matter or goes through a merger, angular momentum is transferred.

The cosmic distribution of black hole spin parameters encodes vital aspects of black hole–galaxy co-evolution, and recent work has been devoted to this topic. Broadly speaking, there are two different suggestions on what the spin distribution should look like. Volonteri et al. (2005) argued that the lifetime of quasars is long enough that the innermost regions of accretion disks typically align with black hole spins, while the direction of the angular momentum of the accreted material is constant throughout the quasar activity. These models predict that most

black holes in quasars should have large spins. Volonteri et al. (2007) also suggest that the evolution of black hole spins, after the quasar epoch, depends on the detailed accretion history, which is linked to the morphology of the host. Volonteri et al. (2007) predict that black holes in elliptical galaxies tend to retain large spins. The distribution of spins for black holes hosted in disk galaxies (e.g., Seyferts) is instead predicted to be much shallower, with a tail extending to low spin values.

Alternatively, it has been suggested that accretion always proceeds via small (and short) uncorrelated episodes ("chaotic accretion," King & Pringle 2006), caused by fragmentation of the accretion disk where it becomes self-gravitating. This scenario implies that black hole spins are very low ($\simeq 0.1$–0.3): accretion of randomly oriented droplets of gas would rapidly spin down any black hole, since counter-rotating material spins black hole down more efficiently than co-rotating material spins them up. To resolve this matter, observational spin constraints are needed from as many SMBHs as possible.

Spectroscopy of Fe K emission lines that are formed in the inner accretion disk provide one way to constrain the spin of a black hole (Miller 2007). These disklines are highly skewed due to relativistic Doppler shifts and gravitational redshifts effects (Laor 1991). Especially if one assumes that the accretion disk extends to the innermost stable circular orbit (ISCO; Bardeen et al. 1972), the extremity of the line shifts at the inner disk can be used to infer the spin of the hole.

In this paper, we report initial constraints on the spin of the SMBH in the Seyfert 1 AGN Fairall 9 ($z = 0.047$), using a relativistic disk line. Compared to other Seyferts, where iron lines have been studied in detail, Fairall 9 is an order of magnitude more massive and more luminous. Its central black hole has a mass of $(2.55 \pm 0.56) \times 10^8\, M_\odot$ based on reverberation mapping (Peterson et al. 2004). The Eddington fraction has been measured to be as high as 0.16 (Done & Gierlinski 2005). Our data reduction procedure is described in

Section 2. A description of the assumptions and various models we used to obtain the spin of Fairall 9 follows in Section 3. In Section 4, we discuss our results and their implications.

2. DATA AND REDUCTION

We observed Fairall 9 with the *Suzaku* X-ray Telescope. The 168 ks run started on 2007 June 7 at 3:34:52 (TT). The data were taken using the X-ray Imaging Spectrometer (XIS) and Hard X-ray Detector (HXD), using the XIS pointing position. The three XIS CCD cameras (XIS0, XIS1, and XIS3) cover 0.2–12.0 keV while the HXD/PIN covers the 10.0–60.0 keV band. The XIS data were taken in both 3×3 and 5×5 binning models. Exposures made using the 3×3 mode lasted 150 ks while the 5×5 exposures lasted approximately for 18.5 ks. The HXD/PIN detector ran in default mode with an exposure time of approximately 136.5 ks.

We reduced the version 2 processed data using the HEASOFT reduction and analysis suite, version 6.4. For the XIS0 and XIS3 cameras, which are front-illuminated CCDs, we extracted source counts from a $3\farcm1$ (180 pixel) region around the center of the source. Background counts were extracted from annuli between $3\farcm1$ and $8\farcm1$ (180–466 pixels). For XIS1, the background was taken from $3\farcm6$ to $8\farcm3$ (212–486 pixels).

We created XIS redistribution matrix files (rmf) and ancillary response files (arf) using the HEASOFT commands "xisrmfgen" and "xissimarfgen," respectively. The arf files were created using a simulation that propagates photons through a model of the telescope; we ran the simulation using the recommended 400,000 photons. Using these files, we grouped the data from each of the 3×3 and 5×5 binning modes to create one spectral file for each of the XIS detectors.

The HXD/PIN spectrum was extracted and corrected for dead time using the standard tools. The dead-time fraction amounted to only a few percent. We then used the non X-ray background file from *Suzaku* that corresponded to our observation to correct its exposure time to match the background. We then modeled the cosmic X-ray background using a response file provided from *Suzaku* for the XIS nominal pointing using XSPEC version 11.3. The corrected non-X-ray background file was added to the simulated cosmic X-ray background file; the combined file served as the background file for analysis of the HXD/PIN spectrum.

In our subsequent analysis of the XIS spectra, we considered the 0.7–10.0 keV range. Above and below this range, strong deviations from reasonable models are found, indicative of calibration uncertainties. In our analysis of the HXD/PIN spectrum, we considered the 12.0–30.0 keV range. Fairall 9 is not clearly detected above 30 keV.

3. ANALYSIS AND RESULTS

We used XSPEC version 11.3 for all of the spectral analysis reported in this work. All errors stated were found using the "error" and "steppar" commands in XSPEC, and correspond to the 1σ level of confidence. The energy of all spectral lines is reported in the source frame, unless otherwise noted. All of the spectral models described below were modified by an interstellar absorption column density set to 3×10^{20} cm^{-2} via the "phabs" model. In all fits, we tied the parameters for all four cameras together but allowed a constant factor to float between the HXD and XIS detectors to account for absolute flux offsets. Our best-fit model (see below) gives a value of 1.16 for the normalizing
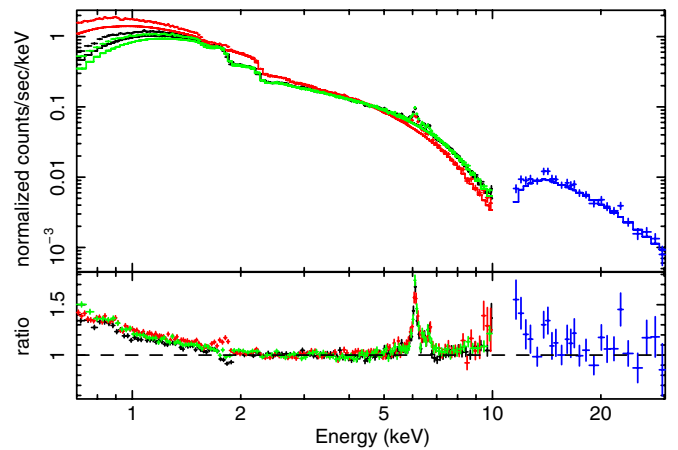

Figure 1. In this figure, the continuum was fitted with a simple power law between 2–3 and 7–10 keV. There is a slight excess seen toward the softer X-rays which can be modeled with a 0.2 keV blackbody. At high energy, some of the flux excess is consistent with disk reflection. The XIS0, XIS1, XIS3, and HXD spectra are shown in black, red, green, and blue, respectively.

constant, consistent with current calibrations (see, e.g., *Suzaku* Memo 2008–06).

We first fit the data with a power law between 2–3 keV and 7–10 keV. The data/model ratio resulting from this initial fit is shown in Figure 1. This exercise revealed several characteristic spectral features. Below 2 keV, there is a soft flux excess that has sometimes been modeled using a $kT = 0.2$ keV blackbody or disk blackbody. Where required, we fit this component with a disk blackbody in the models described below, but we caution that this is a fiducial model to account for the flux, not strong evidence of such a hot disk (see Crummy et al. 2006 for a more physical treatment of the soft excess). Above 9 keV, there is a weak excess above the power law, particularly in the HXD data. This excess is consistent with a Compton-backscattering hump due to disk reflection of the incident hard X-ray flux.

The putative hard flux excess is consistent with the presence of Fe K emission lines, which also arise through reflection. The most prominent emission line is narrow and has a measured energy of 6.10 keV, or 6.40 keV in the frame of Fairall 9 (Figure 2). Narrow Fe Kα lines are common in the X-ray spectra of AGN, and may result from illumination of the "torus" (Nandra 2006). In all models discussed below, we fit this line with a simple Gaussian function of zero width, since the line is not resolved. For consistency, we also fit an Fe Kβ line at the proper energy, and with its flux constrained to be 0.16 times that of the Kα line (Molendi et al. 2003). After these narrow lines are fit, a broad asymmetric line is revealed, consistent with reflection from the inner accretion disk (see Figure 3).

As simple models are easily reproducible, we adopted a simple disk blackbody plus power-law model in order to measure a flux. We measure a 0.5–10.0 keV flux of $4.0(1) \times 10^{-11}$ erg cm^{-2} s^{-1} and a 0.5–30.0 keV flux of $5.9(2) \times 10^{-11}$ erg cm^{-2} s^{-1}. The latter flux corresponds to an X-ray luminosity of $2.6(1) \times 10^{44}$ erg s^{-1}. With the bolometric correction found by Marconi & Hunt (2003), this corresponds to an Eddington fraction of approximately 0.13.

With evidence for disk reflection both in the Fe K band and in hard X-rays, we proceeded to fit the spectrum with common reflection models. The reflection models were convolved with a relativistic line function to account for the relativistic Doppler and gravitational redshifts expected near to the black hole (Brenneman & Reynolds 2006). With the assumption that the
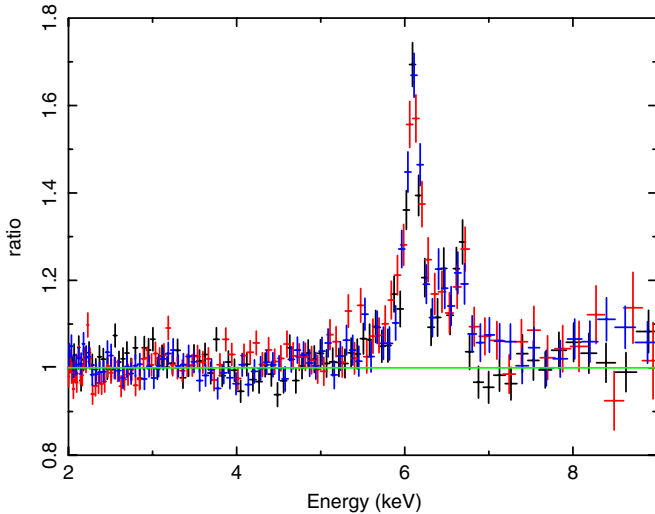
Figure 2. Data/model ratio in Fe K region that results from a simple power-law fit to the data. The narrow Gaussian peak near 6.1 keV (6.4 keV in the rest frame) is due to reflection from distant gas. A broad diskline component is also clearly present. The XIS0, XIS1, and XIS3 spectra are shown in black, red, and blue, respectively.

Figure 3. Data/model ratio in the Fe K region, after fitting the continuum and narrow emission lines. A relativistically broadened diskline is clearly detected. The XIS0, XIS1, and XIS3 spectra are shown in black, red, and blue, respectively.

accretion disk is truncated at the ISCO (consistent with the high Eddington fraction of Fairall 9; also see Miller et al. 2006), the degree to which the line and reflection spectrum are skewed can be used to constrain the spin of the black hole in Fairall 9. These fits are discussed in detail in the following section.

3.1. Neutral Disk Reflection

The "pexrav" model describes the reflection of an exponentially cutoff power-law spectrum from a neutral disk (Magdziarz & Zdziarksi 1995). As noted above, we blurred this spectrum using the "kerrconv" model. Pexrav does not include an emission line, so our spectral model also included the "kerrdisk" line model. Parameters common to the line and convolution blurring function were linked for self-consistency. A fiducial disk blackbody component ("diskbb") was included in the model to account for the soft excess seen in Figure 1.

Pexrav requires the metal abundance in solar units and the iron abundance relative to the metal abundance, as fit parameters. In the absence of observational constraints on elemental abundances in Fairall 9, we fixed the metal abundance to 1.0 and ran the fit three separate times with an iron abundance of 0.5, 1.0, and 2.0 which gave χ^2 values of 6575.3, 6553.7, 6626.3 (respectively) for 5970 degrees of freedom.

Since the relativistic line and disk reflection models are necessarily separate when "pexrav" is employed, the equivalent width of the relativistic line can be measured directly. We find a line equivalent width of $W = 130 \pm 10$ eV. Each fit made with pexrav found Fairall 9 to be consistent with low or moderate spin values. Abundances of 0.5 and 1.0 gave spin values of $a = 0.0^{+0.2}$ and $a = 0.1^{+0.5}_{-0.1}$, respectively. In all cases, maximal spin is excluded at more than the 5σ level of confidence.

Since the convolution model has the inner disk inclination as a variable parameter, while pexrav uses the cosine of that angle, it was not possible to link these two parameters directly. The results discussed above are based on an inclination of $40°$. This value was selected after fitting the model with several different inclination values and tracing the evolution of the goodness-of-fit statistic, and it is in broad agreement with the inclination found using other models (see below).
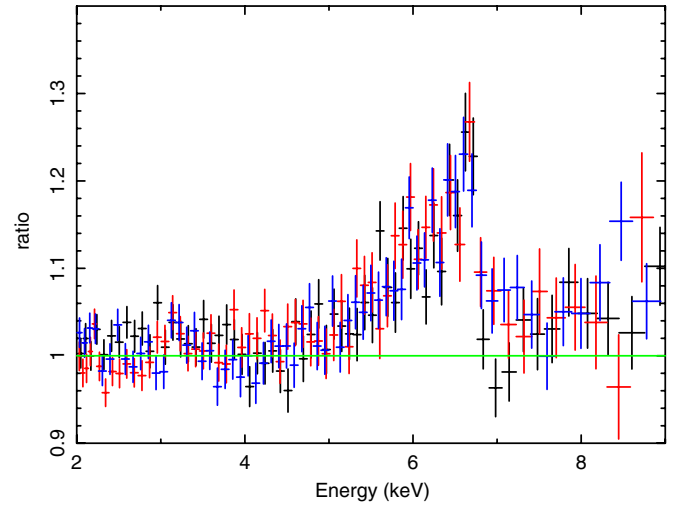
The results we obtained with this model are not entirely self-consistent. A relativistic line centroid energy of $6.70^{+0.01}_{-0.03}$ keV is measured, consistent with He-like Fe xxv. This is at odds with the assumption of a completely neutral accretion disk. Moreover, a reflection fraction of 2.0 is required in all fits. Yet a reflection fraction of $\simeq 0.7$ is suggested by the equivalent width of the relativistic line (George & Fabian 1991).

3.2. Ionized Disk Reflection

Our best fits to the data were obtained using "reflionx" (Ross & Fabian 2005). This model includes an Fe K emission line, a broad range of ionization species, and allows the iron abundance to be a free parameter. Unlike pexrav, it is an angle-averaged model; the inclination angle is not a variable parameter in spectral fits. Owing to the fact that reflionx includes low-energy emission lines that can be blurred into a pseudocontinuum that could be the origin of the soft excess (e.g., Crummy et al. 2006), we did not include a disk blackbody when fitting with reflionx. It should be noted that reflionx requires a photon power-law index as an input but requires a separate power-law component to fit the continuum. Accordingly, we linked the power-law index between the two components. Acceptable fits to Fairall 9 could not be obtained when the Fe abundance and line emissivity parameters were frozen at their nominal values. These parameters were therefore allowed to vary.

With 5970 degrees of freedom, a blurred reflionx model gave a good fit: $\chi^2 = 6498.6$ (see Table 1 and Figure 4). This is significantly better than the fits achieved with the pexrav. Whereas fits with "pexrav" required an ionized line despite the assumption of neutral reflection, "reflionx" returns more self-consistent and reasonable parameter values. A steep line emissivity is required (a maximum of $q = 5$ was fixed as per the case of light bending near to a spinning black hole Miniutti et al. 2003). Using reflionx, we measure a spin of $a = 0.60 \pm 0.07$. A maximal spin is ruled out at the 10σ level of confidence, and zero spin is ruled out at more than the 7σ level of confidence (see Figure 5).

Owing to the fact that CCDs are made of Si, effective area curves often change abruptly in the Si band. This makes it difficult to calibrate detector responses in the Si range. A
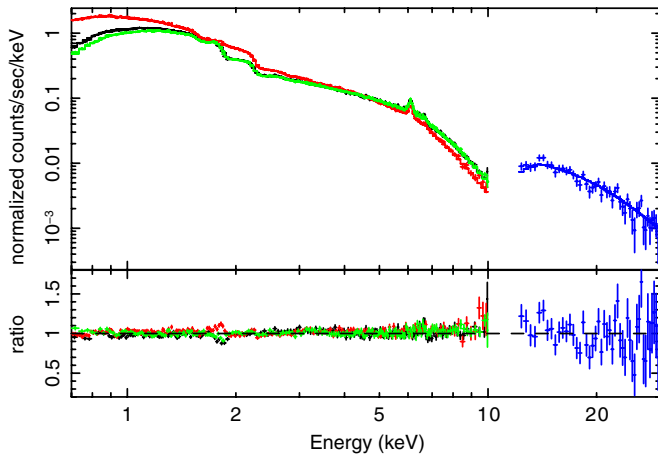
Figure 4. Spectra of Fairall 9 fit with the "reflionx" model and the resultant data/model ratio. This model assumes an ionized disk, but with more ionization species than the CDID model. This model provides the best overall fit to the spectrum of Fairall 9, and suggests a spin of $a = 0.60 \pm 0.07$. The XIS0, XIS1, XIS3, and HXD spectra are shown in black, red, green, and blue, respectively.

Table 1
Summary of Model Parameters

Parameter	Reflionx
Fe K-α narrow line (keV)	$6.400^{+0.002}_{-0.002}$
Fe K-α narrow line norm (10^{-5})	$2.2^{+0.2}_{-0.2}$
Spin (cJ/GM^2)	$0.65^{+0.05}_{-0.05}$
Inclination (deg)	44^{+1}_{-1}
Emissivity index	$5.0_{-0.1}$
Inner radius (R_{ISCO})	$1.0*$
Outer radius (R_{ISCO})	$400.0*$
ξ (erg cm s^{-1})	$3.7^{+0.1}_{-0.1}$
Photon index	$2.09^{+0.01}_{-0.01}$
Fe abundance	$0.8^{+0.2}_{-0.1}$
Reflection norm (10^{-5})	9^{+1}_{-1}
Chi-squared	6503.7
dof	5969

Notes. The parameters of our best-fit relativistically-blurred disk reflection model are given above. Frozen parameters are marked with an asterisk. The normalization of the power-law component external to the "reflionx" model is $8.3(1) \times 10^{-3}$. A hard limit of $q = 5$ was set on the line emissivity index as per Merloni & Fabian (2003). The inner and outer blurring radii correspond to the innermost stable circular orbit (ISCO) for the given spin parameter.

formally acceptable fit with reflionx is not found only due to lingering difficulties in the calibration of the XIS response in the Si band. In Figure 1, clear residuals are seen in this narrowband that differ between the XIS cameras. The residuals do not affect the broadband fit parameters apart from the goodness-of-fit statistic.

To understand the influence of the soft X-ray band on the spin constraint made with "reflionx," we ignored the spectra below 2 keV and performed new error scans on the spin parameter. These fits achieve a significantly worse spin constraint: $a = 0.5^{+0.1}_{-0.3}$. Zero spin is only excluded at the 90% level of confidence; however, maximal spin is excluded at more than the 5σ level.

3.3. Inner Reflections

Though it is common to attribute the spectral features we have observed to X-ray reflection from the inner disk, it is
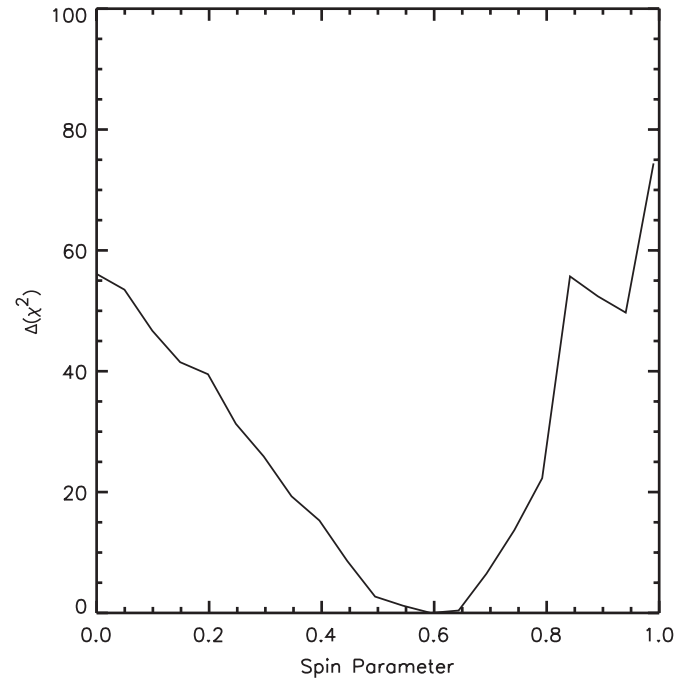

Figure 5. This figure shows how the goodness-of-fit statistic varies with black hole spin, when the spectra of Fairall 9 are fitted with the "reflionx" disk reflection model. Extremal values are clearly excluded by the data.

important to rigorously rule out alternatives. This is especially important in cases like Fairall 9: although the continuum is arguably "simpler" than that of Seyfert 1 AGN that have an X-ray warm absorber (see, e.g., Blustin et al. 2005), the signal to noise ratio in the Fe K band is lower than in cases like MCG-6-30-15 (e.g., Miniutti et al. 2007). We conducted additional investigations to evaluate the robustness of the disk reflection spectrum and relativistic line interpretation.

The spectra shown in Figures 1–3—and evidence for a relativistic disk line—could be biased by the influence of a disk reflection spectrum. We therefore replaced the power-law model used in those figures with a "pexrav" reflection model. The reflection fraction was set to 0.7, which corresponds to the equivalent width of the neutral Fe K line at 6.4 keV ($R =$ EW/180 eV; George & Fabian 1991). Note that this is itself conservative, since the reflection edge is a sharp neutral edge, not one that is broadened by Compton scattering, and the reflection spectrum was not blurred. Two neutral Gaussians corresponding to neutral Fe Kα and Kβ lines were added as before. A poor fit is achieved with this model ($\chi^2/\nu = 6747.4/5975$); broad residuals are still visible in the spectrum (see Figure 6).

Next, two additional narrow Gaussians corresponding to He-like Fe XXV and H-like Fe XXVI were included in the model. These lines were allowed to vary freely in flux. This is a very conservative measure: narrow lines corresponding to Fe XXV or Fe XXVI are extremely rare in surveys of Seyfert 1 X-ray spectra (see, e.g., Nandra et al. 2007). Although this model achieved an improved fit ($\chi^2/\nu = 6689.7/5973$), it still failed to account for all of the flux in the Fe K band (see Figure 6). Brenneman & Reynolds have recently reported evidence for narrow ionized lines in an *XMM-Newton* spectrum of Fairall 9; however, the lines are single-bin features in a snapshot observation spectrum. There is no compelling evidence for distinct lines in our *Suzaku* spectra.

When the two Gaussians corresponding to narrow ionized Fe K lines are replaced with a single Laor line function with
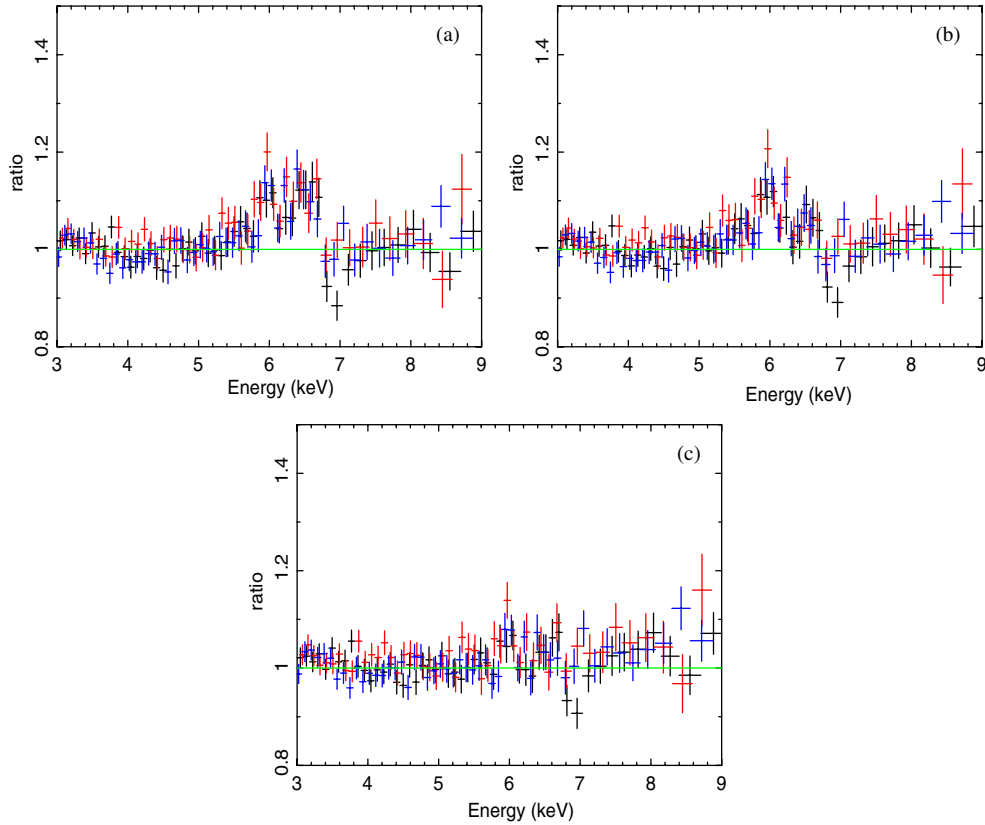
Figure 6. Data/model ratios in this figure show the XIS spectra in the Fe K band (XIS0 in black, XIS1 in red, XIS3 in blue), after fitting the models described in Section 3.3. Panel A shows the data/model ratio in the Fe K band after two neutral Gaussian lines are added to a reflection continuum. Panel B shows the same ratio after two additional Gaussians, corresponding to Fe XXV and XXVI, have been added. Panel C shows the residuals when a single diskline is added instead of two ionized Fe K lines.

reasonable parameters ($R_{in} = 6 \ GM/c^2$, $i = 40°$, $q = 3$), a significantly improved fit is achieved ($\chi^2/\nu = 6628.7/5973$). Moreover, the spectrum through the Fe K band is fit well. An F-test assuming a difference of 1 degree of freedom suggests that the relativistic line model is an improvement over the ionized narrow Gaussians model at the 7σ level of confidence. Compared to just the neutral Gaussians model, the relativistic disk line model represents an improvement at more than the 10σ level of confidence (see Figure 6).

4. DISCUSSION AND CONCLUSIONS

We obtained a deep exposure of the Seyfert AGN Fairall 9 using *Suzaku*. Owing to the sensitivity of the HXD, the source was detected out to 30 keV for the first time. The high-energy spectrum is consistent with disk reflection, commensurate with the broad Fe K line detected in the XIS spectra. We therefore fit the spectra with two different disk reflection spectra, each convolved with a relativistic line function in which the spin of the black hole is a free parameter. With the assumption that the inner edge of the accretion disk extends to ISCO, we are thus able to constrain the spin of the black hole. Our best fit to the spectrum of Fairall 9 using the "reflionx" model suggests $a = 0.60 \pm 0.07$ and excludes extremal spins at a high level of statistical confidence.

We employed a number of steps and tests for the purpose of evaluating the quality of the reflection fit and the robustness of the spin constraint.

1. A model including multiple narrow Gaussians from differ-ent charge states of iron, even when added to a raw reflection

spectrum, achieves a fit that is significantly worse than mod-els with a relativistic line.

2. Fits with a model for reflection from a neutral disk ("pexrav") provided a significantly worse description of the data, but yield spin constraints commensurate with our best-fit model. Pexrav includes a sharp neutral Fe K edge, whereas the spectra appear to require ionized reflection (and a Comptonized edge). Although fits with "pexrav" marked an important test, the model is not ideally suited to the observed spectra.

3. Excluding bins below 2 keV, our best-fit relativistically-blurred ionized disk reflection model ("reflionx") yielded a spin constraint commensurate with that achieved through fits to the full spectral band, though with larger errors. The larger errors are likely the result of two influences: lower overall sensitivity owing to the exclusion of the band with the greatest number of photons, and an inability to detect the soft excess (which may be a psuedocontin-uum of blurred disk emission lines; see Crummy et al. 2006).

A broad Fe K line was previously detected in Fairall 9 using *ASCA* (Reynolds 1997). More recently, a short *XMM-Newton* observation did not achieve the sensitivity required to detect such a feature (Gondoin et al. 2001; also see Brenneman & Reynolds 2009). A broad Fe K line is not only detected in our *Suzaku* spectra, but was easily separated from distinct narrow lines and shown to be asymmetric and therefore consistent with a disk origin. This was possible because of the resolution of the XIS CCDs and the sensitivity achieved in our long exposure. Of the sources wherein relativistic disk lines have been detected

(see, e.g., Miller 2007 and Nandra et al. 2007), Fairall 9 is among the most massive (Peterson et al. 2004).

Our results add to a preliminary picture suggesting that there may be a range of black hole spin parameters even within a rather homogeneous class of AGNs. Brenneman & Reynolds (2006) have reported a spin approaching $a \simeq 0.99$ in the Seyfert 1 AGN MCG-6-30-15 (Reynolds & Fabian 2008 suggest that systematics could bring the spin down to $a = 0.92$), and Miniutti et al. (2009) have reported a spin parameter of $a = 0.6 \pm 0.2$ in the narrow-line Seyfert 1 AGN SWIFT J2127.4+5654. These results are self-consistent in that they all derive from spectral fits with relativistically-blurred disk reflection models. A similar picture may be emerging from studies of stellar mass black holes (Miller et al. 2009).

In each of these three cases, a steep line emissivity ($q \simeq 5$) is required. This value is consistent with theoretical predictions of the influence of gravitational light bending near to a spinning black hole (Miniutti et al. 2003). However, MCG-6-30-15 is the only case among the three wherein a high spin parameter has been inferred. The proper form of the emissivity index is largely unknown, at present. In the case of Fairall 9, the emissivity index could be as high as $q = 6$, though an upper bound of $q = 5$ is enforced in our fits. (The spin constraints are consistent for $q = 5$ and $q = 6$). Observations of microlensing in quasars indicates that the hard X-ray emission region is smaller than $6GM/c^2$ (Chartas et al. 2009). Such results bolster implications for light bending and steep line emissivity parameters.

A range of spin parameters is allowed by current theoretical investigations. Based on calculations performed by Berti & Volonteri (2008) that take into consideration both black hole mergers and accretion onto black holes, the probability of a spin as high as that of MCG-6-30-15 is less than 10^{-4} in the chaotic accretion model. Alternatively, if accretion occurs in a coherent fashion, the spin distribution should peak at high value (e.g., $a \geqslant 0.9$). However, the predicted distributions have a small tail extending to zero spin: the probability of a spin < 0.1 in the coherent accretion scenario is 10%. Volonteri et al. (2007) also discuss how the distribution of spins in low-redshift AGN is likely broader than the theoretical limit derived for quasars in the coherent accretion model, which requires galaxy mergers to drive large gas inflows and to trigger quasar activity. Thus, the fact that our models imply that the black hole in Fairall 9 may have a moderate spin is consistent with current theories.

However, with only three spin constraints, we cannot yet rule out any of the theoretical models, despite their striking differences. Many more spin constraints are needed to distinguish between different predictions of the cosmological black hole spin distribution (Volonteri et al. 2005; King & Pringle 2006). Our results demonstrate that the sensitivity and resolution of the XIS cameras, and the sensitivity and low background of the HXD, are extremely helpful in measuring disk reflection spectra. Over the lifetime of the *Suzaku* mission, spin constraints may be possible in as many as 20 Seyfert AGNs. In the long run, the much larger collecting area of the *International X-ray Observatory* will make it possible to obtain spin measurements in as many as 300 AGN (Brenneman et al. 2009).

REFERENCES

Bardeen, J. M., Press, W. H., & Teukolsky, S. A. 1972, ApJ, 178, 347
Berti, e., & Volonteri, M. 2008, ApJ, 684, 822
Blandford, R. D., & Znajek, R. L. 1977, MNRAS, 179, 433
Blustin, A. J., Page, M. J., Fuerst, S. V., Branduardi-Raymont, G., & Ashton, C. E. 2005, A&A, 431, 111
Brenneman, L. W., & Reynolds, C. S. 2006, ApJ, 652, 1028
Brenneman, L. W., & Reynolds, C. S. 2009, ApJ, 702, 1367
Brenneman, L. W., et al. 2009, Astro2010 Science White Paper (arXiv: 0902.4691)
Chartas, G., Kochanek, C. S., Dai, X., Poindexter, S., & Garmire, G. 2009, ApJ, 693, 174
Crummy, J., Fabian, A. C., Gallo, L. C., & Ross, R. R. 2006, MNRAS, 365, 1067
Done, C., & Gierlinski, M. 2005, MNRAS, 364, 208
Fabian, A. C., et al. 2002, MNRAS, 335, L1
George, I. M., & Fabian, A. C. 1991, MNRAS, 249, 352
Gondoin, P., Lumb, D., Siddiqui, H., Guainazzi, M., & Schartel, N. 2001, A&A, 373, 805
King, A. R., & Pringle, J. E. 2006, MNRAS, 373, L90
Laor, A. 1991, ApJ, 376, 90
Larsson, J., Miniutti, G., Fabian, A. C., Miller, J. M., Reynolds, C. S., & Ponti, G. 2008, MNRAS, 384, 1316
Magdziarz, P., & Zdziarksi, A. A. 1995, MNRAS, 273, 837
Marconi, A., & Hunt, L. K. 2003, ApJ, 589, L21
Merloni, A., & Fabian, A. C. 2003, MNRAS, 342, 951
Miller, J. M. 2007, ARA&A, 45, 441
Miller, J. M., et al. 2006, ApJ, 653, 525
Miller, J. M., et al. 2009, ApJ, 697, 900
Miniutti, G., Fabian, A. C., Goyder, R., & Lasenby, A. N. 2003, MNRAS, 344, L22
Miniutti, G., Panessa, F., de Rosa, A., Fabian, A. C., Malizia, A., Molina, M., Miller, J. M., & Vaughan, S. M. 2009, MNRAS, 398, 255
Miniutti, G., et al. 2007, PASJ, 59, 315
Molendi, S., Bianchi, S., & Matt, G. 2003, MNRAS, 343, L1
Nandra, K. 2006, MNRAS, 368, L62
Nandra, K., et al. 2007, MNRAS, 382, 194
Peterson, B. M., et al. 2004, ApJ, 613, 682
Reynolds, C. S. 1997, MNRAS, 286, 513
Reynolds, C. S., & Fabian, A. C. 2008, ApJ, 675, 1048
Ross, R. R., & Fabian, A. C. 1993, MNRAS, 261, 74
Ross, R. R., & Fabian, A. C. 2005, MNRAS, 358, 211
Sikora, M., Stawarz, L., & Lasota, J.-P. 2007, ApJ, 658, 815
Thorne, K. 1974, ApJ, 191, 507
Volonteri, M., Madau, P., Quataert, E., & Rees, M. J. 2005, ApJ, 620, 69
Volonteri, M., Sikora, M., & Lasota, J.-P. 2007, ApJ, 667, 704